Middle Viséan (Mississippian) coral biostrome in central Guizhou, southwestern China and its palaeoclimatological implications

Le Yao[a,b*], Xiangdong Wang[a], Wei Lin[a], Yue Li[a], Steve Kershaw[c], Wenkun Qie[a]

[a] *LESP and LPS, Nanjing Institute of Geology and Paleontology, Chinese Academy of Sciences, Nanjing 210008, China*

[b] *University of Chinese Academy of Sciences, Beijing, 100049, China*

[c] *Department of Life Sciences, Brunel University, Uxbridge, Middlesex, UB8 3PH, UK*

* Correspondence should be addressed to Le Yao, E-mail: yaole010081@163.com

Abstract

A middle Viséan (Mississippian) coral biostrome is reported for the first time from the Shangsi Formation in Yashui area, central Guizhou Province, southwestern China (palaeogeographically located in eastern Palaeotethys). The biostrome, which is about 500 m across and 2.5-3.9 m thick, is laterally variable and composed of rugose and tabulate corals with low taxonomic diversity comprising 4 rugose and 1 tabulate coral species belonging to 5 genera. Three growth stages of the biostrome are distinguished, based on different compositions of coral taxa. Average coral contents of the biostrome increase from 38.7% to 72.0% upward and the main builders are *Siphonodendron pentalaxoidea*, *Syringopora* sp. and *Kueichouphyllum sinense*. Associated fossils include abundant brachiopods, crinoids and common foraminifers together with rare calcareous algae, bryozoans, gastropods and ostracods. Relative sea-level changes are interpreted to have controlled growth and demise of the biostrome, which grew continuously during sea-level rise and decreasing water energy, as evident from the gradually increasing of micrite content and *in situ* coral colonies. However, the biostrome declined and died as the sea level fell and hydrodynamic energy strengthened, indicated by an increase of bioclasts and sparry calcite cement (indicating lack of micritic matrix due to higher energy) overlying the biostrome. This coral biostrome has similar biotic composition to middle to late Viséan coral biostromes in Europe and North Africa (western Palaeotethys). The approximately coeval occurrence of coral

biostromes in both eastern and western Palaeotethys suggest that a relatively global warm episode existed during the Viséan Stage.

Keywords: coral biostrome, composition, growth and demise, middle Viséan, southwestern China

1. Introduction

The Mississippian was an important interval for reef evolution when skeletal bioconstructions recovered after collapse of the coral-stromatoporoid reefal ecosystem during the Frasnian-Famennian (F-F) mass extinction event (Copper, 2002; Webb, 2002; Wang and Shen, 2004; Aretz and Chevalier et al., 2007). During the Famennian, a microbial reefal ecosystem replaced the metazoan reefal ecosystem and only few stromatoporoid reefs and stromatoporoid-coral biostromes were present (Webb, 2002; Wang and Shen, 2004; Aretz and Chevalier et al., 2007). In the Tournaisian Stage, no skeletal bioconstructions have been reported but Waulsortian mud mounds were widely developed (Lees and Miller, 1985; Wang and Shen, 2004). Thus the loss of reef-building metazoans resulted in buildups that lack skeletal bioconstructions (Wang and Shen, 2004) and climate cooling is likely to have played a part in the delayed recovery of reef-building metazoans (e.g. Isbell et al., 2003; Buggisch et al., 2008; Grossman et al., 2008; Yao et al., 2015). The Viséan Stage (hereafter abbreviated to Viséan) was a recovery period of skeletal bioconstructions when sponge-bryozoan-coral reefs and biostromes developed (Webb, 2002), consistent with flourishing metazoan builders (Wang and Shen, 2004) and climate warming (e.g. Isbell et al., 2003; Fielding et al., 2008; Grossman et al., 2008; Isbell et al., 2012).

Viséan skeletal bioconstructions have been documented in Western Europe (Adams, 1984; Bancroft et al., 1988; Aretz and Herbig, 2003a, b; Chevalier and Aretz, 2005; Denayer and Aretz, 2012), North Africa (Aretz and Herbig, 2008; Rodríguez et al., 2012), Australia (Webb, 1999), North America (Dix and James, 1987) and Eastern Asia (Antoshkina, 1998; Nakazawa, 2001). They first appeared in the early Viséan with low abundance and were characterized by coral reefs. In the middle Viséan, the abundance of skeletal bioconstructions increased and they were dominated by coral reefs/biostromes and bryozoan reefs. Coral reefs/biostromes, sponge reefs/biostromes and bryozoan reefs were the main components and their abundance shifted to

maximum value during the late Viséan (Webb, 2002). Corresponding to the evolution of skeletal bioconstructions during the Viséan, coral biostromes also recovered and flourished during this time. They were widely distributed in Western Europe and North Africa (western Palaeotethys), including Belgium (Aretz, 2001, 2002), Ireland (Somerville et al., 2007; Aretz et al., 2010), Spain (Rodríguez, 1996), England (Aretz and Nudds, 2007) and Morocco (Said et al., 2010; Rodríguez et al., 2013). Thus, biostromes appeared first in the middle Viséan and gradually increased to peak value during the late Viséan (Aretz and Chevalier et al., 2007). Although the diversity of the biostromes changes from low to high, their major compositions are typified by high abundance of the genus *Siphonodendron* with lower abundance of tabulate and solitary rugose corals.

In South China (eastern Palaeotethys), Viséan skeletal bioconstructions were recorded only in Guangxi Province (Gong et al., 2010; 2012), as bryozoan-coral reefs and coral reefs in Langping County, western Guangxi (Fang and Hou, 1986; Chen et al., 2013). However, the accurate ages of them are unknown, resulting in difficulty to compare them with global skeletal bioconstructions.

Prior to this study, no Viséan coral biostromes have been reported in South China. Their compositions and relationships to coeval coral biostromes in western Palaeotethys are also not understood. In this study, a coral biostrome in the Shangsi Formation is described for the first time in the Yashui (YS) area in Huishui County, central Guizhou Province, southwestern China (Fig. 1a, b). In total, three locations of the biostrome have been found, exposed at YS-A, YS-B and YS-C sections (Fig. 1c). The present study aims to (1) assess the biotic compositions and their lateral and vertical variations in the biostrome; (2) interpret the environmental factors controlling the growth and demise of the biostrome; (3) compare Viséan coral biostromes worldwide and provide insights into their palaeoclimatological significance.

2. Geological setting

2.1. Palaeogeography

During the Viséan, the South China Block (SCB) was located near the equator in northeastern Palaeotethys (Fig. 2 a), which implies that the climate of SCB was warm during this time. The SCB displays a variety of sedimentary facies (Fig. 2 b) (Feng et al., 1998). A large-scale

carbonate platform (the Dian-Qian-Gui-Xiang (DQGX) platform) existed in the southern part of SCB (Fig. 2B) and was characterized by shallow-water sediments, which provided a suitable environment for the development of skeletal bioconstructions. The Qian-Gui (QG) Basin is an intra-platform basin in the central part of the DQGX platform, constrained by NE-SW and NW-SE trending rifts and lithologically dominated by black shales, thin- bedded limestones and siliceous rocks (Jiao et al., 2003). A narrow nearshore siliciclastic belt extended between the DQGX platform and the southern Yangtze and western Cathaysia contemporary landmasses (Feng et al., 1998). In this study, the YS-A, YS-B and YS-C sections are located on the margin of the DQGX platform towards the QG Basin and far from ancient landmasses (Fig. 2 b).

2.2. Lithostratigraphy

In South China, correlations of the Mississippian strata and their relations with those in Belgium via foraminiferal zones (MFZ) were summarized by Wang and Jin (2000) and Hance et al. (2011). These Chinese rock sequences were formerly called the Fengningian Subsystem and subdivided into the Tangbagouan stage of the Aikuanian Series and Jiusian, Shangsian and Dewu stages of the Tatangian Series in ascending order (Fig. 2 c). Five lithological units in Yashui are (from base to top): Tangbagou, Xiangbai, Jiusi, Shangsi and Baizuo formations (Feng et al., 1998) (Fig. 2c), which are approximately equivalent to MFZ1-MFZ6 (Hastarian-Lower Ivorian substage), MFZ7-MFZ8 (Upper Ivorian substage), MFZ9-MFZ12 (Molinacian-Livian substage), MFZ13-MFZ15 (Warnantian-Pendleian substage), MFZ16 (Arnsbergian substage), respectively (Somerville, 2008; Hance et al., 2011; Aretz et al., 2014). The formations comprise abundant limestones rich in shelly fossils implying a shallow marine environment favorable for skeletal bioconstructions where there is less terrestrial input. The coral biostrome is exposed at the base of the Shangsi Formation (Wu, 1987) (Fig. 2 d).

Exposures of the upper part of the Jiusi Formation to the lower part of the Shangsi Formation are well exposed in the YS-A, YS-B and YS-C sections (Fig. 3 a, b, c). The upper part of the Jiusi Formation consists of dark-gray thin- to medium-bedded (0.1~0.5 m) bioclastic limestones intercalated with dark shales containing diverse assemblages of brachiopods, corals, foraminifers, crinoids, calcareous algae, gastropods, bryozoans and ostracods (Wu, 1987). The lower part of the

Shangsi Formation is composed of dark-gray medium- to thick-bedded (0.3~1.2 m) bioconstructional limestones, bioclastic limestones and cherty limestones yielding abundant corals, foraminifers, brachiopods, crinoids, calcareous algae, and rare gastropods, bryozoans and ostracods (Wu, 1987).

In the YS-A, YS-B and YS-C sections, the coral biostromes are clearly distinguished by the higher abundance of *in situ* corals (Fig. 3). The underlying limestones are mainly composed of dark-grey thick-bedded packstones with few solitary rugose corals, colonial rugose corals and tabulate corals, which provide a substrate for coral colonization (Fig. 4 a).

In the YS-A and YS-C sections, the coral biostrome is about 3.2 m and 3.9 m thick respectively and mainly composed of dark-gray thick-bedded solitary rugose coral, colonial rugose coral and tabulate coral bafflestones and framestones (Yao et al., 2014) (Fig. 4 b, c, d). Variation in abundance of biostrome builders allows the recognition of three vertical growth stages, stage 1, stage 2 and stage 3, in ascending order. Stage 1 contains abundant solitary rugose corals with few tabulate corals (Fig. 4 b). Stage 2 has solitary rugose corals and tabulate corals as the main components (Fig. 4 c). Stage 3 is mostly comprised of colonial rugose corals with few solitary rugose corals and tabulate corals (Fig. 4 d).

At YS-B section, the coral biostrome is about 2.5 m thick and consists of solitary rugose coral and tabulate coral bafflestones and framestones. Compared with the YS-A and YS-C sections, the YS-B section lacks the growth stage of colonial rugose corals (stage 3), which may be caused by the random colonization of colonial rugose corals on top of the biostrome forming local patch reefs. Only the two lower growth stages have been developed (Fig. 3 b).

The boundary between the coral biostrome and its overlying limestones have been identified at the three studied sections. the boundary is characterized by irregular surfaces indicating a slight positive topographic relief (Fig. 4 e, f) and the overlying limestones are characterized by light-grey thin-bedded packstones with sparse solitary rugose corals, altogether indicating demise of the biostrome (Fig. 4 e, f).

2.3. Biostratigraphy

In South China, the Shangsi Formation is generally consistent with the *Yuanophyllum* Zone

(Yü, 1933), the base of which is equivalent to the RC6 rugose coral Zone of the middle Viséan in Europe (Poty et al., 2006). In this study, the coral biostrome is located at the base of the Shangsi Formation (Wu, 1987), suggesting that the biostrome is of middle Viséan age. Also, the occurrence of the foraminifers in the coral biostrome and its overlying limestones, such as *Pojarkovella nibelis*, *Koskinobigenerina breviseptata* and *K. cribriformis*, indicates that it belongs to the MFZ12 foraminiferal Zone in the middle Viséan, which is equivalent to Livian substage in Belgium and Holkerian substage in Britain (Poty et al., 2006; Somerville, 2008; Hance et al., 2011).

3. Materials and methods

Altogether 66 large samples (about 10×20 cm) and 84 solitary rugose corals were collected through the sequence, from thin-bedded muddy limestones underlying the biostrome to the thin-bedded packstones overlying the biostrome at YS-A, YS-B and YS-C sections. 238 thin sections (10×10 mm, 15×25 mm, 40×50 mm and 70×100 mm sized) for coral identifications and 197 thin sections (40×50 mm sized) and 24 polished slabs (about 10×15 cm) for microfacies analysis were prepared with orientations. The quantitative analysis of the coral content of the biostrome is based on the point-counting method proposed by Webb (1999) and Wen and Liu (2009). In each stage of the biostrome, a well exposed, relatively flat and smooth surface with adequate area was chosen for the appropriate grid analysis (Webb, 1999). The selected surfaces were uniformly covered by about 500 points and the point distance was about 5 cm. Then, the points covering corals were counted. Quantitative analysis of the different genera contents of the solitary rugose corals is obtained from the counting of each coral genera based on a large number of samples from uniform collecting. The semi-quantitative analysis of the contents of the biostrome-dwellers is conducted by detailed observation of thin sections under microscope. Identifications of microfacies types of the biostrome and its underlying and overlying limestones follow the classification schemes proposed by Dunham (1962) and Embry and Klovan (1971).

4. Results

4.1. Biotic compositions of the coral biostrome

175 *4.1.1. Coral biostrome-builders*

176 The coral biostrome contains high abundance of (more than 60%) coral skeletons in place in
177 the YS-A, YS-B and YS-C sections (Fig. 4 b, c, d). It is defined here as an autobiostrome
178 following the biostrome classification scheme of Kershaw (1994). However, the diversity of
179 fossils in the biostrome is quite low and only five species have been recognized, which are the
180 solitary rugose *Arachnolasma irregulare* Yü, 1933, *Bothrophyllum longiseptatum* Lewis, 1931
181 and *Kueichouphyllum sinense* Yü, 1931, the colonial rugose *Siphonodendron pentalaxoidea* Yü,
182 1933, and the tabulate *Syringopora* sp.

183 Quantitative analysis for the three studied sections show that the coral abundance increases
184 from stage 1 to stage 3 (Fig. 5 a). In stage 1, the coral abundances are 45.0%, 41.0% and 30.0% in
185 the YS-A, YS-B and YS-C sections respectively and the average coral content is 38.7% (Fig. 5 a,
186 6 a). Stage 1 is dominated by *K. sinense* with less *Syringopora* sp. and *B. longiseptatum*, and their
187 contents are 62.2%, 15.6% and 22.2% in the YS-A section, 48.8%, 24.4% and 26.8% in the YS-B
188 section and 41.7%, 41.7% and 16.6% in the YS-C section (Fig. 5 b). The average contents of them
189 are 54.2%, 23.2% and 22.6% (Fig. 6 b). In Stage 2, the coral contents increase to 63.0%, 48.6%
190 and 44.5% with an average value of 52.0% (Fig. 5 a, 6 a). Stage 2 is mainly composed of *K.*
191 *sinense* and *Syringopora* sp., which make up 44.6% and 46.8% in the YS-A section, 58.4% and
192 33.7% in the YS-B section and 67.4% and 32.6% in the YS-C section (Fig. 5 b). The mean values
193 of the genera contents are 53.3% and 38.7% for *K. sinense* and *Syringopora* sp., respectively (Fig.
194 6 b). Scarce *A. irregulare*, *B. longiseptatum* and *S. pentalaxoidea* also occurred in this stage (Fig.
195 5 b, 6 b). In Stage 3, the coral contents with peak values of 75% and 68% are presented in the YS-
196 A and YS-C sections respectively and the average value is 72% (Fig. 5 a, 6 a). Stage 3 is largely
197 comprised of *S. pentalaxoidea*; it occupies 90% in the YS-A section and 95.6% in the YS-C
198 section with an average value of 92.7% (Fig. 5 b, 6 b). A few *K. sinense*, *B. longiseptatum* and
199 *Syringopora* sp. was also present in this stage (Fig. 5 b, 6 b). From the quantitative analysis of the
200 coral contents, the compositions of the corals vary both laterally and vertically implying biotic
201 heterogeneity of the biostrome, which is typical of skeletal bioconstructions.

202

203 *4.1.2. Coral biostrome-dwellers*

Associated fossils of the coral biostrome are abundant and diverse in spaces between skeletons of biostrome-builders in the YS-A, YS-B and YS-C sections (Fig. 7) (Table 1). In the field, brachiopods, crinoids and gastropods were found in the biostrome. From the observation of thin sections, the biostrome-dwellers also contain foraminifers, calcareous algae (e.g. palaeoberesellids), bryozoans (e.g. fenestellids, cryptostomes and trepostomes) and ostracods (Fig. 7). The occurrence of the palaeoberesellids in the biostrome implies shallow water photic settings (Gallagher, 1998). The abundance of the dwellers gradually decreases from stage 1 to stage 3. Although the diversity and abundance of biostrome-dwellers is variable in the biostrome, there is similar composition of associated fossils in the each stage across the three sections (Table 1). In stage 1 and 2, diverse bioclasts are present including brachiopods, crinoids, foraminifers, calcareous algae, bryozoans, gastropods and ostracods. Among the bioclasts, brachiopods are abundant, crinoids are common and foraminifers are common in stage 1 and rare in stage 2. Calcareous algae, bryozoans, gastropods and ostracods are usually rare throughout these two stages except some of them are occasional common in some locations (Table 1). The diversity and abundance of the biostrome-dwellers declined distinctly in stage 3. They contain brachiopods (common), and rare crinoids, foraminifers, calcareous algae and bryozoans (Table 1). For the studied sections, the differences in the composition of biostrome-dwellers between the three stages reflect the temporal and spatial changes in the biotic constitutions of the biostrome. The occurrence of diverse associated fossils between the skeletons of biostrome-builders suggests that the biostrome had a stable and healthy ecosystem.

4.2. Morphological and taphonomical variations of corals

Morphological and taphonomic variations of corals in the coral biostrome are significant palaeoecological parameters. Most corals of the biostrome are preserved apparently in place, with very few coral fragments (Fig. 8). Generally, solitary rugose corals have three growth orientations (parallel, inclined and vertical to stratification). Tabulate corals are small clusters or have a ribbon form. Colonial rugose corals commonly grew in inclined or upright fasciculate form with asexual budding structures. In stage 1, solitary rugose corals are mainly distributed parallel to the substrate. Most of them are separated from each other and few solitary rugose corals are attached with each

other (Fig. 8 a). Tabulate corals are mostly located between the skeletons of the solitary rugose corals in small clusters. Few of them are distributed around or in contact with solitary rugose corals. Tabulate corals are mostly disintegrated into individual corallites (Fig. 8 a). Solitary rugose corals of stage 2 are also characterized by horizontally preserved form, but the content of the attached form increases (Fig. 4 c, 8 b). During this stage, tabulate corals are mainly represented by ribbon form in the space between the skeletons of solitary rugose corals, which are in contact with few tabulate corals. Compared with stage 1, many more corallites and colonies of the tabulate corals connect with their neighbours in stage 2 (Fig. 8 b). Colonial rugose corals are scattered between the skeletons of solitary rugose and tabulate corals during this stage (Fig. 8 c). In stage 3, most colonial rugose corals are inclined or upright in fasciculate form (Fig. 4 d). Cross sections of them in the surface of polished slabs suggests that they grew in the same direction. In this stage, colonial rugose corals are mostly attached to each other with asexual budding structure (Fig. 4 d, 8 d). Among the skeletons, scarce solitary rugose and tabulate corals are distributed with horizontal or inclined form and small clusters, respectively. In stage 1, the individual solitary rugose and tabulate corals with mainly horizontal and small cluster forms reflect the initial simple growth forms of the biostrome-builders, indicating the framework of the biostrome was not rigid. During stage 2, the increasing connectedness of the solitary rugose corals and tabulate corals with major ribbon form suggests that more complicated growth forms of the biostrome-builders (implying a more solid framework) were formed during this time. In stage 3, mostly attached colonial rugose corals with asexual budding structure, which are preserved in inclined or upright fasciculate form, indicate that the bioconstructions of the biostrome-builders are mature with a relatively rigid framework.

4.3. Microfacies analysis

Microfacies types (Table 1) include bioclastic wackestones, bioclastic packstones, bioclastic floatstones, bafflestones and framestones (Fig. 9, 10 a, b, c, d). Sedimentary structures comprise geopetal structures, burrows and borings (Fig. 10 e, f, g, h). In the underlying limestones, the microfacies types are characterized by bioclastic packstones with abundant burrows and rare borings (Table 1). In the biostrome, the microfacies types of stage 1 are dominated by bafflestone

with rare framestone and bioclastic floatstone. Bioclastic wackestone and packstone is common between skeletons of biostrome-builders. Burrows are common while borings and geopetal structures are relatively rare during this stage (Table 1). In stage 2, the microfacies types are mainly composed of bafflestone and framestone with rare bioclastic floatstone. Bioclastic wackestone is abundant between skeletons of builders. Burrows are also common with rare geopetal structures (Table 1). During stage 3, the microfacies types are largely comprised of bafflestone and framestone with rare bioclastic floatstone. Burrows, borings and geopetal structures are rare during this time (Table 1). In the overlying limestones, the microfacies is bioclastic packstone with rare burrows (Table 1).

4.3.1. Microfacies types

Bafflestone

Bafflestones are abundant in the coral biostrome, which are formed by *in situ* preserved corals (Fig. 9 a, b, c) (Table 1). In the space between the corals, micrites and bioclasts were deposited, presumed baffled by the corals where water energy was reduced. The corals forming such bafflestones are *Syringopora*, *Kueichouphyllum*, *Bothrophyllum* and *Arachnolasma* in stage 1 and 2, *Siphonodendron* in stage 3.

Framestone

This microfacies type is common in the coral biostrome and characterized by the attached framework of corals, interpreted as wave-resistant (Fig. 9 b, c, d) (Table 1). The interspace between corals is filled with peloids, micrites and bioclasts where water energy is presumed to have been greatly decreased. *Siphonodendron*, *Syringopora* and *Kueichouphyllum* are commonly closely packed together forming framestone.

Bioclastic floatstone

Compared with bafflestone and framestone, bioclastic floatstone is rare in the coral biostrome (Table 1). Within these bioclastic floatstones, calcareous algae, bryozoans and microbes commonly encrust the external surfaces of colonial rugose and tabulate corals, and may have

reinforced their wave-resistance (Fig. 9 e, f, g, h). The morphologies of calcareous algae, bryozoans and microbes are irregular developing into filiform, fishtail or globular masses, which are different from the colonies in coverstones with regular flat tabular shape (Cuffey, 1985).

Bioclastic wackestone

Bioclastic wackestone is commonly recognized in the interspace between coral skeletons in the biostrome (Fig. 10 a) (Table 1). They are composed of diverse fossils including common brachiopods, crinoids and foraminifers with rare calcareous algae (e.g. palaeoberesellids), bryozoans, gastropods and ostracods. Bioclasts comprise about 20-35% in volume. They are commonly poorly sorted with slight-breakage. Peloids and micrites fill up the spaces between the bioclasts without obvious cementation.

Bioclastic packstone

This microfacies type is rare in the biostrome while abundant in the underlying and overlying limestones (Table 1). Bioclastic packstone is characterized by abundant and diverse reworked bioclasts with poor-sorting and high-breakage: crinoid ossicles, foraminifers, brachiopods fragments, calcareous algae, bryozoans, gastropods and ostracods (Fig. 10 b, c, d). However, the biotic components are distinctly different between the underlying and overlying limestones. In the underlying limestones, bioclasts are relatively diverse including abundant brachiopod debris, calcareous algae, crinoid ossicles and foraminifers with rare coral fragments, bryozoans, gastropods and ostracods, which are up to 65-75% in volume (Fig. 10 b). In the overlying limestones, crinoid ossicles and foraminifers are the major components with few brachiopods (as debris), calcareous algae (e.g. palaeoberesellids) and ostracods, which make up to 70-80% of the total components (Fig. 10 c, d). Spaces between bioclasts are full of micrite with partial cementation in the YS-A and YS-B sections and sparry calcite with less micrite in the YS-C section (Fig. 10 c, d).

4.3.2. Sedimentary structures

Geopetal structures

Geopetal structures are rare in the coral biostrome and formed within the cavities of brachiopods, gastropods, ostracods and corals (Fig. 10 e) (Table 1).

Burrows

Burrows are generally common in the biostrome and its underlying limestones (Fig. 10 f) (Table 1). They are long columns, elliptical and curving in shapes. The burrows are about 2-3.5 mm in width and mostly filled by sand-sized bioclasts such as crinoid ossicles, brachiopod debris and bryozoan fragments cemented by sparry calcite, silt-sized bioclasts, and micrites. It is remarkable that spindle-shaped opaque pellets concentrate near the burrows. These pellets are epigranular and about 0.2 mm in diameter with a distinct margin, and be the fecal pellets of invertebrates such as worms and gastropods (Lu and Sang, 2002) that may have formed the burrows.

Borings

In the coral biostrome, borings are rarely present compared with burrows (Table 1). They are characterized by different shapes of cavities in coral skeletons (Fig. 10 g, h). Within the cavities of borings, fecal pellets and burrows are commonly present, indicating that they might also be formed by some benthic fauna such as worms or gastropods. On the other hand, the borings provide a residence place for some associated fossils (Fig. 10 g). In addition, some cavities of solitary rugose corals are resided by colonial rugose corals implying that the corals also supply hard substrata for further coral colonization (Fig. 10 h).

5. Discussion

5.1. Controlling factors of growth and demise of the coral biostrome

Bioconstructions form a complex ecosystem controlled by numerous intrinsic and extrinsic factors including palaeobiology and palaeoenvironment (Aretz and Chevalier, 2007). During the Viséan, sea-level changes frequently occurred (Haq and Schutter, 2008). According to the litho-

and biofacies analysis of coral biostromes in the middle to late Viséan, growth and demise of the biostromes are interpreted here to be mainly controlled by changes of hydrodynamic energy related to sea-level variations (Rodríguez, 1996; Aretz, 2001, 2002; Aretz and Nudds, 2007; Somerville et al., 2007; Aretz et al., 2010; Said et al., 2010).

In this study, the controlling factors of the growth and demise of the coral biostrome are interpreted from the sedimentological and biotic characters of the biostrome and its underlying and overlying strata. For the YS-A, YS-B and YS-C sections, in the underlying limestones, the microfacies are mainly bioclastic packstones in which the bioclasts are usually poorly sorted and show high-breakage (Fig. 10 b). They are likely to have been transported in relatively high-energy conditions unsuitable for coral growth (Said et al., 2010; Yao et al., 2014) (Fig. 11 a) and then deposited. Only few solitary rugose, colonial rugose and tabulate corals grew during this time (Fig. 4 a). From stage 1 to stage 3 of the biostrome, microfacies types gradually changed from bioclastic wackestones and packstones to bioclastic wackestones with increasing abundance of peloids and micrites and decreasing of bioclasts (Fig. 9 b, c, 10 a) (Table 1). Also, during stage 1 and stage 2, solitary rugose corals are usually preserved horizontally and lack erect growth forms (Fig. 4 b, c, 8 a, b). In stage 3, the colonial rugose corals of *Siphonodendron* are mostly upright or inclined in fasciculate form (Fig. 4 d, 8 d). They are very similar to the growth form of the corals in the *Siphonodendron* biostromes in Belgium, Ireland and Spain, which usually grew in a depth between the fair-weather wave-base and storm wave-base (Rodríguez, 1996; Aretz, 2001, 2002; Somerville et al., 2007) (Table 2). Furthermore, the coral abundance in the biostrome distinctly increases from stage 1 to stage 3 (Fig. 5 a). The characteristics of both microfacies and corals in the biostrome suggest that a weaker hydrodynamic condition developed for the growth of *in situ* coral assemblages in a depth between the fair-weather wave-base and storm wave-base driven by continuous sea-level rise (Fig. 11 b). In the overlying limestones, the microfacies type is dominated by bioclastic packstone with an increase of bioclasts and sparry calcite (Fig. 10 c, d). Such microfacies characteristics indicate that the hydrodynamic energy strengthened due to the dramatic fall of sea-level, which is interpreted here to have caused the demise of the biostrome (Fig. 11 c).

5.2. Comparisons

Middle to late Viséan coral biostromes have been reported in Europe (Belgium, England, Ireland and Spain) and North Africa (Morocco), which were located in western Palaeotethys during this time (Fig. 12) (Rodríguez, 1996; Aretz, 2001, 2002; Aretz and Nudds, 2007; Somerville et al., 2007; Aretz et al., 2010; Said et al., 2010). The types of the biostromes vary from parabiostrome to autobiostrome (Kershaw 1994) (Table 2). The thickness of the biostromes is different ranging from thin to very thick (0.2-50m) and their lateral extension vary from some tens of meters to several kilometers. The diversity of the biostromes also changes from low to high, but the major components are commonly dominated by the lower diversity of the genus *Siphonodendron* (mainly *S. junceum*, *S pauciradiale* and *S. martini*) (Table 2). Diverse solitary rugose corals are presented in *Siphonodendron* biostromes including the genera of *Arachnolasma*, *Axophyllum*, *Aulophyllum*, *Caninophyllum*, *Clisiophyllum*, *Dibunophyllum*, *Haplolasma*, *Koninckophyllum*, *Palaeosmilia*, *Pseudozaphrentoides* and *Siphonophyllia*. The biostrome-dwellers commonly contain brachiopods, crinoids, foraminifers, calcareous algae, bryozoans, gastropods and ostracods (Table 2). In this study, the occurrence of the coral biostrome in South China Block (eastern Palaeotethys) provides an excellent example to study its comparisons with the coral biotromes from western Palaeotethys (Fig. 12).

Three thin- to medium-thickness *Siphonodendron* biostromes have been reported from the middle to upper Viséan bioclastic limestones in Belgium (Aretz, 2001, 2002) (Table 2). Middle Viséan biostromes were exposed in the sections of Engihoul, Corphalie, Bomel and Polderlee and mainly constructed by *S. martini*. Solitary and colonial rugose corals are rare (Aretz, 2002) (Table 2). Two late Viséan biostromes were developed in Royseux, southeast Belgium (Aretz, 2001). The lower biostrome is dominated by *S. junceum* with scattered *Lithostrotion maccoyanum*, *S. pauciradiale*, *Syringopra* sp. and no solitary rugose corals. The upper biostrome is mainly constructed by *S. junceum* in the lower part and *S. martini* in the upper part. Solitary rugose corals include *Aulophyllum*, *Dibunophyllum* and *Koninckophyllum*. Distinctly different from the *martini* biostromes, the *S. junceum* and *S. martini* corals of the *junceum* and *junceum-martini* biostromes are mostly in growth position with low fragmentation (Table 2).

Siphonodendron biostromes of the late Viséan were also recorded in southeastern and

northwestern Ireland (Somerville et al., 2007; Aretz et al., 2010). The biostromes in SE Ireland are dominated by *S. pauciradiale* in life position and characterized by cyclic cessation in growth (Somerville et al., 2007). *S. pauciradiale*, *S. martini* and *S. junceum* coralla are the major components of the biostromes in NW Ireland (Caldwell and Charlesworth, 1962; Aretz et al., 2010). The *pauciradiale* and *martini* biostromes have a lower proportion of *in situ* colonies than that of the *junceum* biostromes. Compared with the biostromes in Belgium, solitary rugose corals are obviously more abundant in the biostromes of Ireland containing *Axophyllum*, *Aulophyllum*, *Caninophyllum*, *Clisiophyllum*, *Dibunophyllum*, *Haplolasma*, *Palaeosmilia*, *Pseudozaphrentoides* and *Siphonophyllia* (Table 2).

Late Viséan *Siphonodendron* biostromes were also described from the Sierra Morena area of southwestern Spain (Rodríguez et al., 1994; Rodríguez, 1996) with many similarities to those of SE Ireland in biostromal type and biotic compositions (Somerville et al., 2007). However, in SW Spain, the dominant colonial rugose corals of the biostromes are the larger-sized species of *S. martini* or *S. irregulare* (Rodríguez, 1996) (Table 2).

At Little Asby Scar, northern England, a late Viséan coral-chaetetid sponge biostrome has been studied by Aretz and Nudds (2007), and is composed of chaetetid-dominated facies alternating with coral-dominated facies. The coral-dominated facies mainly consist of *Siphonodendron* coral debris making up about 95% in volume, which provide a hard substrate for chaetetid sponge growth. The *Siphonodendron* biostrome lacks colonies in growth position (< 2.5%) which is distinctly different from the other coral biostromes developed in Europe. The solitary rugose corals are composed of *Axophyllum*, *Caninophyllum* and *Siphonophyllia* (Table 2).

A late Viséan coral biostrome was also documented from Adarouch area in central Morocco, North Africa, which has a close relationship to the coral biostromes in Europe (Said et al., 2010). The dominant species of the biostrome is *in situ* preserved *S. junceum* with similar solitary rugose coral fauna such as *Axophyllum*, *Clisiophyllum*, *Dibunophyllum* and *Palaeosmilia* (Table 2).

The coral biostrome in South China shows some similarities to those in Europe and North Africa in terms of the biotic composition of biostrome-builders and -dwellers (Table 2). In this study, more than 60% corals of the biostrome are preserved in place, which could be classified as autobiostrome (Kershaw, 1994). The biostrome has a low diversity including 5 coral species

436 belonging to 5 genera. *Siphonodendron* genera are one of the main components in the biostrome
437 studied here, which are also the dominant species of the biostromes in Europe and North Africa
438 (Table 2). Another major component of *Syringopora* is also presented in the *Junceum* and
439 *Siphonodendron* biostromes in Belgium and Spain respectively (Rodríguez, 1996; Aretz, 2001). In
440 the *Siphonodendron* limestones, *Siphonodendron* corals are commonly in growth position with
441 little breakage, which is also an obvious characteristic of the biostromes in Europe and North
442 Africa (Table 2). The biostrome-dwellers are diverse including brachiopods, crinoids, foraminifers,
443 calcareous algae, bryozoans, gastropods and ostracods, which are also the common associated
444 biota in the biostromes of Europe and North Africa (Table 2).

445 Although the coral biostromes in Europe and North Africa have diverse solitary rugose corals,
446 they are not the most abundant species in the biostromes. In South China, the coral biostrome also
447 has solitary rugose corals, such as *Kueichouphyllum*, *Bothrophyllum* and *Arachnolasma*. The
448 genus *Kueichouphyllum* is also a major component of the biostrome but is absent in the
449 biostromes of Europe and North Africa (Table 2). The palaeobiogeographic distribution (Niikawa,
450 1994) of *Kueichouphyllum* explains its abundance in South China and its absence in European
451 reefs. Different compositions of the solitary rugose corals in the coral biostromes between Europe
452 and North Africa and South China may be ascribed to their different locations of
453 palaeobiogeography with different ocean circulation and climate.

454

455 *5.3. Coral biostrome evolution and paleoclimatological significance*

456 Reef ecosystems were severely affected by retreats during mass extinction events (Copper,
457 1988; Kiessling, 2001). It is not surprising that the coral-stromatoporoid reefal ecosystems
458 collapsed during the F-F mass extinction event (Copper, 2002; Wang and Shen, 2004), replaced
459 by microbial communities such as stromatolites, thrombolites and mud mounds in the Famennian
460 and Tournaisian (Lees and Miller, 1985; Webb, 2002; Wang and Shen, 2004). Skeletal
461 bioconstructons did not re-appear until the early Viséan and their abundance gradually increased
462 to peak value during the late Viséan, when corals, bryozoans and sponges were the major builders
463 (Webb, 2002). In the Viséan, as a special skeletal bioconstruction, coral biostromes also recovered
464 and flourished in Europe and North Africa consistent with the other skeletal bioconstructions

(Rodríguez, 1996; Aretz, 2001, 2002; Aretz and Nudds, 2007; Somerville et al., 2007; Aretz et al., 2010; Said et al., 2010). They first appeared in the middle Viséan with a low abundance and increased in abundance during the late Viséan. In this study, the development of the coral biostrome in South China during the middle Viséan indicates that the evolution of the coral biostrome in South China was consistent with that of Europe and North Africa (Fig. 12).

The microfacies types of the coral biostrome consist of bafflestones and framestones which are also the typical microfacies in organic reefs (Flügel, 2004). In the biostrome, the reproduction of colonial rugose corals is featured by asexual budding (Fig. 4 d), which is a very important mode for the construction of organic reefs during Phanerozoic time (Fagerstrom and West, 2011), such as the coral reefs in modern Caribbean Sea (Foster et al., 2007). The occurrence of bafflestones, framestones and asexual budding in the coral biostrome suggests that the biostrome has the lithological and biotic characteristics of organic reefs. However, compared with structures of biohermal organic reefs, the biostrome lacks binders and cementation that would have strengthened frameworks. The litho- and bio-characterisics of the biostrome presented in this study reflect that of the initially recovered coral biostromes during the Viséan.

The Mississippian Epoch is a critical interval in geological history, when the transition from Devonian greenhouse climate to Permo-Carboniferous icehouse climate is generally interpreted (Young, 1991; Grossman, 2012; Yao et al., 2015). According to the published studies, glacial deposits developed during the Tournaisian and Serpukhovian stages accompanied by low abundance of reef-builders (Isbell et al., 2003; Wang and Shen, 2004; Fielding et al., 2008; Isbell et al., 2012), which may have impeded the evolution of skeletal bioconstructions (Webb, 2002; Wang and Shen, 2004). In the Viséan, the resurgence of skeletal bioconstructions is interpreted as a function of reef-builders flourishing and climate warming (Webb, 2002; Wang and Shen, 2004). Consistent with the recovery of skeletal bioconstructions in the Viséan, coral biostromes also developed and gradually flourished from the middle to late Viséan in Europe and North Africa (western Palaeotethys). Combined with the coral biostromes in western Palaeotethys, the occurrence of coral biostromes in South China (eastern Palaeotethys) suggests that the abundance of corals increased and a relatively global warm episode did exist during the Viséan compared with the cold climate in the Tournaisian and Serpukhovian.

6. Conclusions

(1) A middle Viséan coral biostrome is documented for the first time from southwestern China, in the Shangsi Formation in Yashui area, central Guizhou. It is composed mainly of the genera *Siphonodendron*, *Syringopora* and *Kueichouphyllum* with lesser abundance of *Bothrophyllum* and *Arachnolasma*. Biostrome-dwellers are diverse including abundant brachiopods and crinoids and common foraminifers with rare calcareous algae, bryozoans, gastropods and ostracods. The microfacies types of the biostrome are mainly composed of bafflestone, framestone and bioclastic wackestone. Compared with biohermal organic reefs, the biostrome lacks binders and cementation.

(2) Ecological successions have been observed in the coral biostrome. In the underlying limestones of the biostrome, the abundant and diverse bioclasts with few solitary rugose, colonial rugose and tabutale corals provide a substrate for coral colonization. In the biostrome, three growth stages have been distinguished, which are *Kueichouphyllum sinense* growth stage, *K. sinense* -*Syringopora* sp. growth stage and *Siphonodendron pentalaxoidea* growth stage. YS-A and YS-C sections show the three growth stages, while YS-B section lacks the *S. pentalaxoidea* growth stage.

(3) The variations of hydrodynamic energy due to sea-level changes controlled the growth and demise of the coral biostrome. The development of the biostrome is attributed to gradual sea-level rise and weakened hydrodynamic energy, as evident from the presence of abundant micrites and *in situ* coral colonies. The biostrome is interpreted to have died as sea-level fell and hydrodynamic energy strengthened, indicated by increasing abundance of bioclasts and sparry calcite cement.

(4) The coral biostrome shows some similarities to coeval cases in Europe and North Africa in aspects of the dominant biostrome-builders such as *Syringopora* and *Siphonodendron*, and their associated fossils. The occurrence of *Kueichouphyllum* in the biostrome, which is absent in Europe and North Africa during the Viséan, may be ascribed to their different locations of palaeobiogeography. During the middle to late Viséan, the occurrence of coral biostromes in both South China (eastern Palaeotethys) and Europe and North Africa (western Palaeotethys) suggest that a relatively global warm episode did exist during this time.

Acknowledgments

This manuscript was greatly improved by the comments from Prof. F.T. Fürsich of Erlangen University and Dr. J.T Chen of Nanjing Institute of Geology and Paleontology. We would like to give our thanks to Drs. Yuping Qi and Zhaoliang Ma for their help in the fieldwork. This work was financially supported by National Natural Science Foundation of China (grant Nos.: 41290260, 41290262) and the Ministry of Science and Technology Foundation Project.

References

Adams, A.E., 1984. Development of algal-foraminiferal-coral reefs in the Lower Carboniferous of Furness, northwest England. Lethaia 17, 233-249.

Antoshkina, A.I., 1998. Organic buildups and reefs on the Palaeozoic carbonate platform margin, Pechora Urals, Russia. Sediment. Geol. 118, 87-211.

Aretz, M., 2001. The upper Viséan coral-horizons of Royseux-the development of an unusual facies in Belgian Early Carboniferous. Tohoku Univ. Mus. Bull 1, 86-95.

Aretz, M., 2002. Habitatanalyse und Riffbildungspotential kolonialer rugoser Korallen im Unterkarbon (Mississippium) von Westeuropa. Kölner Forum für Geologie und Paläontologie 10, 1-155.

Aretz, M., Herbig, H.-G., 2003a. Coral-Rich Bioconstructions in the Viséan (Late Mississippian) of Southern Wales (Gower Peninsula, UK). Facies 49, 221-242.

Aretz, M., Herbig, H.-G., 2003b, Contribution of rugose corals to Late Viséan and Serpukhovian bioconstructions in the Montagne Noire (Southern France). In: Ahr, W.M., Harris, P.M., Morgan, W.A., Somerville, I.D. (Eds.), Permo-Carboniferous Carbonate Platforms and Reefs, Society for Economic Palaeontologists and Mineralogists Special Publication 78, and American Association of Petroleum Geologists Memoir 83, pp. 119-132.

Aretz, M., Chevalier, E., 2007. After the collapse of stromatoporid-coral reefs-the Famennian and Dinantian reefs of Belgium: much more than Waulsortian mounds. In: Álvaro, J.J., Aretz, M., Boulvain, F., Munnecke, A., Vachard, D., Vennin, E. (Eds.), Palaeozoic Reefs and Bioaccumulations: Climatic and Evolutionary Controls. Geological Society, London, Special Publications 275, pp. 163-188.

552 Aretz, M., Nudds, J., 2007. Palaeoecology of the Late Viséan (Dinantian) coral-chaetetid
553 biostrome at Little Asby Scar (Cumbria, Great Britain). In: Hubmann, B., Piller, W.E. (Eds.),
554 Fossil corals and sponges: Schriftenreihe der Erdwissenschaftlichen Kommissionen der
555 Österreichischen Akademie der Wissenschaften 17, pp. 365-381.
556 Aretz, M., Herbig, H.-G., 2008. Microbial-sponge and microbial metazoan buildups in the
557 Late Viséan basin-fill sequence of the Jerada Massif (Carboniferous, NE Morocco). Geol. J. 43,
558 307-336.
559 Aretz, M., Herbig, H.-G., Somerville, I.D., Cózar, P., 2010. Rugose coral biostromes in the
560 late Viséan (Mississippian) of NW Ireland: Bioevents on an extensive carbonate platform.
561 Palaeogeogr. Palaeoclimatol. Palaeoecol. 292, 488-506.
562 Aretz, M., Nardin, E., Vachard, D., 2014. Diversity patterns and palaeobiogeographical
563 relationships of latest Devonian-Lower Carboniferous foraminifers from South China: What is
564 global, what is local? J. Palaeogeogr. 3, 35-59.
565 Bancroft, A.J., Somerville, I.D., Strank, A.R.E., 1988. A bryozoan buildup from the Lower
566 Carboniferous of North Wales. Lethaia 21, 1-65.
567 Buggisch, W., Joachimski, M.M., Sevastopulo, G., Morrow, J.R., 2008. Mississippian
568 $\delta^{13}C_{carb}$ and conodont apatite $\delta^{18}O$ records-Their relation to the Late Palaeozoic Glaciation.
569 Palaeogeogr. Palaeoclimatol. Palaeoecol. 268, 273-292.
570 Caldwell, W.G.E., Charlesworth, H.A.K., 1962. Viséan coral reefs in the Bricklieve
571 Mountains of Ireland. Proceedings of the Geologists' Association 73, 359-382.
572 Chen, X.H., Gong, E.P., Wang, T.H., Guang, C.Q., Zhang, Y.L., Yang, D.Y., Wang, H.M.,
573 2013. The basic characteristics of Early Carboniferous coral reef at Xiadong village in Tianlin,
574 Guangxi, and its sedimentary environment. Acta Geol. Sin. 87, 597-608.
575 Chevalier, E., Aretz, M., 2005. A microbe-bryozoan reef from the Middle Viséan of the
576 Namur Syncline (Engihoul Quarry). Geol. Belg. 8, 109-119.
577 Copper, P., 1988. Ecological Succession in Phanerozoic Reef Ecosystems: Is It Real? Palaios
578 3, 136-151.
579 Copper, P., 2002. Silurian and Devonian reefs: 80 million years of global greenhouse
580 between two ice ages. In: Kiessling, W., Flugel, E., Golonka, J. (Eds), Phanerozoic reef patterns.

SEPM Special Publication 72, pp. 181-238.

Cuffey, R.J., 1985. Expanded reef-rock textural classification and geological history of bryozoans reefs. Geology 13, 307-310.

Denayer, J., Aretz, M., 2012. Discovery of a Mississippian Reef in Turkey: The Upper Viséan Microbial-Sponge-Bryozoan-Coral Bioherm From Kongul Yayla (Taurides, S Turkey). Turk. J. Earth Sci. 21, 375-389.

Dix, G.R., James, N.P., 1987. Late Mississippian bryozoan/microbial build-ups on a drowned karst terrain: Port au Port Peninsula, western Newfoundland. Sedimentology 34, 779-793.

Dunham, R.J., 1962. Classification of carbonate rocks according to depositional texture. In: Ham, W.E. (Eds.), Classification of Carbonate rocks. American Association of Carbonate Petrologists Memoir 1, 108-122.

Embry, A.F., Klovan, J.E., 1971. A Late Devonian reef tract on Northeastern Banks Island，Northwest Territories. B. Can. Petrol. Geol. 19, 730-781.

Fagerstrom, J.A., West, R.R., 2011. Roles of clone-clone interactions in building reef frameworks: principles and examples. Facies 57, 375-394.

Fang, S.X., Hou, F.H., 1986. The Carboniferous sedimentary environments and the bryozoan-coral patch reef of the Datang age of the Langping carbonate platform in Tianlin county, Guangxi province. Acta Sediment. Sin. 4, 30-42.

Feng, Z.Z., Yang, Y.Q., Bao, Z.D., 1998. Lithofacies paleogeography of the Carboniferous in South China. J. Palaeogeogr. 1, 75-86.

Flügel, E., 2004. Microfacies of carbonate rocks. Springer, Berlin, pp. 1-976.

Fielding, C., Frank, T., Birgenheier, L., Rygel, M.C., Jones, A.T., Roberts. J., 2008. Stratigraphic imprint of the Late Palaeozoic Ice Age in eastern Australia: A record of alternating glacial and nonglacial climate regime. J. Geol. Soc. 165, 129-140.

Foster, N.L., Baums, I.B., Mumby, P.J., 2007. Sexual versus asexual reproduction in an ecosystem engineer: the massive coral Montastraea annularis. J. Anim. Ecol. 76, 384-391.

Gallagher, S.J. 1998. Controls on the distribution of calcareous foraminifera in the Lower Carboniferous of Ireland. Mar. Micropaleontol. 34, 187-211.

Gong, E.P., Zhang, Y.L., Guang, C.Q., Chang, H.L., 2010. Main features of the

610 Carboniferous organic reefs in the world. J. Palaeogeogr. 12, 127-139.

611 Gong, E.P., Zhang, Y.L., Guang, C.Q., Chen, X.H., 2012. The Carboniferous reefs in China.
612 J. Palaeogeogr. 1, 27-42.

613 Gradstein, F.M., Ogg, J.G., Schmitz, M., Ogg, G.A. (eds.), 2012. Geologic Time Scale 2012.
614 Cambridge University Press, London, 2 vols.

615 Grossman, E.L., Yancey, T.E., Jones, T.E., Bruckschen, P., Chuvashov, B., Mazzullo, S.J.,
616 Mii, H.S., 2008. Glaciation, aridification, and carbon sequestration in the Permo-Carboniferous:
617 The isotopic record from low latitudes. Palaeogeogr. Palaeoclimatol., Palaeoecol. 268, 222-233.

618 Grossman, E.L., 2012. Oxygen isotope stratigraphy, in Gradstein, F.M., Ogg, J.G., Schmitz,
619 M., Ogg, G.A. (eds.), Geologic Time Scale 2012. Cambridge University Press, London, pp. 1-206.

620 Hance, L., Hou, H.F., Vachard, D., 2011. Upper Famennian to Visean Foraminifers and
621 Some Carbonate Microproblematica from South China-Hunan, Guangxi and Guizhou. Geological
622 Publishing House, Beijing, pp. 1-359.

623 Haq, B.U., Schutter, S.R., 2008. A chronology of Paleozoic sea-level changes. Science 322,
624 64-68.

625 Isbell, J.L., Miller, M.F., Wolfe, K.L., Lenaker, P.A., 2003. Timing of late Paleozoic
626 glaciation in Gondwana: Was glaciation responsible for the development of Northern Hemisphere
627 cyclothems? Geological Society of America Special Paper 370, 5-24.

628 Isbell, J.L., Henry, L.C., Gulbranson, E.L., Limarino, C.O., Fraiser, M.L., Koch, Z.J.,
629 Ciccioli, P.L., Dineen, A.A., 2012. Glacial paradoxes during the late Paleozoic ice age: Evaluating
630 the equilibrium line altitude as a control on glaciation. Gondwana Res. 22, 1-19.

631 Jiao, D.Q., Ma, Y.S., Deng, J., Meng, Q.F., Li, D. H., 2003. The sequence-stratigraphic
632 framework and the evolution of palaeogeography for Carboniferous of the Guizhou and Guangxi
633 areas. Geoscience 17, 294-302.

634 Kershaw, N., 1994. Classification and geological significance of biostromes. Facies 31, 81-
635 92.

636 Kiessling, W., 2001. Phanerozoic reef trends based on the Paleoreefs database. In: Stanley,
637 G.D. (Eds.), The History and Sedimentology of Ancient Reef Systems. New York, Plenum Press,
638 pp. 41-88.

639 Lees, A., Miller, J., 1985. Facies variations in Waulsortian buildups: part 2. Mid-Dinantian
640 buildups from Europe and North America. Geol. J. 20, 159-180.
641 Lewis, H.P., 1931. On the Carboniferous coral Pseudocaninia (stuckenberg) and
642 Pseudocaninia longisepta, sp.n. The Annals and Magazine of Natural History 7, 225-235.
643 Lu, F.X., Sang, L.K., 2002. Petrology. Geological Publishing House, Beijing, pp. 193-193.
644 Nakazawa, T., 2001. Carboniferous Reef Succession of the Panthalassan Open-Ocean
645 Setting: Example from Omi Limestone, Central Japan. Facies 44, 183-210.
646 Niikawa, I., 1994. The palaeobiogeography of *Kueichouphyllum*. In: Oekentorp-Küster, P.
647 (Eds.), Proceedings of the Ⅵ. International Syposium on Fossil Cnidaria and Porifera. Courier
648 Forschungsinstitut Senckenberg 172, 43-50.
649 Poty, E., Devuyst, F.-X., Hance, L., 2006. Upper Devonian and Mississippian foraminiferal
650 and rugose coral zonations of Belgium and northern France: a tool for Eurasian correlations. Geol.
651 Mag. 143, 829-857.
652 Rodríguez, S., Arribas, M.E., Falces, S., Morena-Eiris, E., de la Pena, J., 1994. The
653 *Siphonodendron* limestone of the Los Santos de Maimona basin: development of an extensive
654 reef-flat during the Viséan in Ossa Morena, Spain. Courier Forschungsinstitut Senckenberg 172,
655 203-214.
656 Rodríguez, S., 1996. Development of coral reef-facies during the Viséan at Los Santos de
657 Maimona, SW Spain. In: Strogen, P., Somerville, I.D., Jones, G.Ll. (Eds.), Recent Advances in
658 Lower Carboniferous Geology: Geological Society Special Publication 107, pp. 145-152.
659 Rodríguez, S., Somerville, I.D., Said, I., Cózar, P., 2012. Late Viséan coral fringing reef at
660 Tiouinine (Morocco): implications for the role of rugose corals as building organisms in the
661 Mississippian. Geol. J. 47, 462-476.
662 Rodríguez, S., Said, I., Somerville, I.D. & Cózar, P., 2013. An upper Viséan (Asbian-
663 Brigantian) and Serpukhovian coral succession at Djebel Ouarkziz (northern Tindouf Basin,
664 southern Morocco). Riv. Ital. Paleont. Stratigr. 119, 3-18.
665 Said, I., Rodríguez, S., Berkhli, M., Cózar, P., Gómez-Herguedas, A., 2010. Environmental
666 parameters of a coral assemblage from the Akerchi Formation (Carboniferous), Adarouch Area,
667 central Morocco. J. Iber. Geol. 36, 7-19.

668 Somerville, I.D., Cózar, P., Rodríguez, S., 2007. Late Viséan rugose coral faunas from south-
669 eastern Ireland: composition, depositional setting and palaeoecology of *Siphonodendron*
670 biostromes. In: Hubmann, B. Piller, W.E. (Eds.), Fossil Corals and Sponges, Proceedings of the
671 9th International Symposium on Fossil Cnidaria and Porifera, Graz, 2003. Austrian Academy of
672 Sciences, Schriftenreihe der Erdwissenschaftlichen Kommissionen 17, Vienna, 307-328.
673 Somerville, I.D., 2008. Biostratigraphic zonation and correlation of Mississippian rocks in
674 Western Europe: some case studies in the late Viséan/Serpukhovian. Geol. J. 43, 209-240.
675 Wang, X.D., Jin, Y.G., 2000. An Outline of Carboniferous Chronostratigraphy. J. Stratigr. 24,
676 90-98.
677 Wang, X.D., Shen, J.W., 2004. The extinction and recovery of reefs from Late Devonian to
678 Early Carboniferous in South China. In: Rong, J.Y., Fang, Z.J. (Eds.), Biological mass extinction
679 and recovery: Implications from the evidences of Palaeozoic and Triassic in South China. Press of
680 University of Science and Technology of China, Hefei, pp. 367-380.
681 Wang, X.D., Qie, W.K., Sheng, Q.Y., Qi, Y.P., Wang, Y., Liao, Z.T., Shen, S.Z., Ueno, K.,
682 2013. Carboniferous and Lower Permian sedimentological cycles and biotic events of South China.
683 Geological Society, London, Special Publications 376, 33-46.
684 Webb, G.E., 1999. Youngest Early Carboniferous (Late Viséan) shallow-water patch reefs in
685 Eastern Australia (Rockhampton Group, Queensland): Combining quantitative micro- and macro-
686 Scale data. Facies 41, 111-140.
687 Webb, G.E., 2002. Latest Devonian and Early Carboniferous reefs: depressed reef building
688 after the Middle Paleozoic collapse. In: Kiessling, W., Flugel, E., Golonka, J. (Eds), Phanerozoic
689 reef patterns. SEPM Special Publication 72, 239-270.
690 Wen, J.J., Liu, J.B., 2009. Quantitative studies of bioclastic grains in carbonate rocks:
691 Theoretical analysis and application of point-counting method. J. Palaeogeogr. 11, 1-12.
692 Wu, X.H., 1987. Carboniferous and Permian Stratigraphy in Guizhou. 11th International
693 Congress of Carboniferous Stratigraphy and Geology, Guide Book, Excursion 5, pp. 17-21.
694 Yao, L., Wang, X.D., Li, Y., Qie, W.K., Lin, W., 2014. Microfacies of the reef and bank
695 limestones from the Lower Carboniferous Shangsi Formation in Huishui, South Guizhou. Geol.
696 Rev. 60, 1381-1392.

Yao, L., Qie, W.K., Luo, G.M., Liu, J.S., Algeo, T.J., Bai, X., Yang, B., Wang, X.D., 2015. The TICE event: Perturbation of carbon–nitrogen cycles during the mid-Tournaisian (Early Carboniferous) greenhouse-icehouse transition. Chem. Geol. 401, 1-14.

Young, G.M., 1991. The geological record of glaciation: Relevance to the climatic history of earth. Geosci. Can. 18, 100-108.

Yü, C.C., 1931. The correlation of the Fengning System, the Chinese Lower Carboniferous, as based on coral zones. Bulletin of the Geological Society of China 10, 1-30.

Yü, C.C., 1933. Lower Carboniferous corals of China. Palaeontologia Sinica, Ser. B 12, pp. 1-211.

Figure captions

Fig. 1. (a) Location of Guizhou Province in China. (b) Location of the study section, (the shadow area of Fig. 1 (a)). (c) Enlargment of the shadow area of Fig. 1 (b) showing positions of the studied YS-A, YS-B and YS-C sections containing coral biostromes.

726 Fig. 2. (a) Global palaeogeography of the late Mississippian (340 Ma) (after
727 http://jan.ucc.nau.edu/~rcb7/RCB.html, courtesy of Ron Blakey). The black rectangle represents
728 the inset map in panel b; note that the South China craton was rotated ~90^0 counter-clockwise
729 relative to its modern orientation. SB: South China Block. (b) The Viséan-Serpukhovian
730 paleogeography of South China Block (after Feng et al., 1998) and the location of the studied
731 sections. DQGX: Dian-Qian-Gui-Xiang platform; QG: QianGui basin. (c) The stratigraphic
732 framework of the Mississippian in South China and Yashui (Guizhou Province), respectively
733 (modified from Wang and Jin, 2000, Gradstein et al., 2012 and Wang et al., 2013). (d) The Viséan
734 geological map of the studied area (derived from Wu, 1987).
735
736 Fig. 3. Field photographs and lithologic columns of the coral biostrome and its underlying and
737 overlying strata in the YS-A, YS-B and YS-C sections. (a) Field photograph of the coral
738 biostrome in the YS-A section containing three growth stages. (b) Field photograph of the coral
739 biostrome in the YS-B section including two growth stages. (c) Field photograph of the coral
740 biostrome in the YS-C section containing three growth stages. S: shale, M: muddy limestone, W:
741 wackestone, P: packstone, G: grainstone, R: rudstone, B: biostrome, NE: North-east direction, NW:
742 North-west direction, ENE: East-north east direction.
743
744 Fig. 4. Field photographs of the coral biostrome and its underlying and overlying limestones in the
745 YS-A and YS-B sections. (a) Underlying limestones with few solitary rugose corals in the YS-A
746 section. (b) Solitary rugose coral and tabulate coral bafflestones of stage 1 in the YS-A section. (c)
747 Solitary rugose coral and tabulate coral bafflestones and framestones of stage 2 in the YS-A
748 section. (d) Colonial rugose coral bafflestone and framestone of stage 3 in the YS-A section. (e)
749 The boundary between stage 3 and its overlying limestone in the YS-A section. (f) The boundary
750 between stage 2 and its overlying limestone in the YS-B section. AB: Asexual budding, CR:
751 Colonial rugose coral, SR: Solitary rugose coral, T: Tabulate coral.
752
753 Fig. 5. Composition of the coral biostrome and corals in the biostrome in the YS-A, YS-B and YS-
754 C sections. (a) Coral content of the biostrome. (b) Coral genus content in the biostrome.

Fig. 6. (a) Average coral content of the biostrome classified in broad groups. (b) Average coral genera content of the corals in the biostrome.

Fig. 7. Thin-section micrographs of biostrome-dwellers. (a) Fenestellid bryozoans, foraminifers and calcareous algae (palaeoberesellids) in the coral biostrome. (b) Cryptostome bryozoans, crinoids, calcareous algae (palaeoberesellids) and ostracods in the biostrome. (c) Brachiopods and trepostome bryozoans in the biostrome. (d) Brachiopods and gastropods in the biostrome. Bra: Brachiopod, Bry: Bryozoan, C: Crinoids, Cr: Cryptostome, F: Foraminifer, Fe: Fenestellid, G: Gastropod, O: Ostracod, P: Palaeoberesellid, SC: Solitary rugose coral, Si: *Siphonodendron*, Tr: trepostome.

Fig. 8. Polished slabs show morphological and taphonomical variations of corals in the coral biostrome in the YS-A and YS-B sections. (a) The separated solitary rugose corals mainly preserved parallel to stratification with few tabulate corals attached, and the tabulate corals grow in small clusters and are mostly disintegrated into individual corallites in stage 1 in the YS-A section. (b) Most of the solitary rugose corals are also preserved parallel to stratification wih few tabulate corals connected, but the contents of tabulate corals greatly increase with more corallites and colonies connected with their neighbours and distributed by ribbon form during stage 2 in the YS-A section. (c) The scattered distribution of colonial rugose corals in the interplace between the solitary rugose corals and tabulate corals in stage 2 in the YS-B section. (d) The attached colonial rugose corals grew in inclined or upright fasciculate form with same cross sections on the surface of the polished slab. SR: Solitary rugose coral, CR: Colonial rugose coral, T: Tabulate coral. All scale bars are 1 cm.

Fig. 9. Thin-section micrographs of the microfacies types in the coral biostrome. (a) *Kueichouphyllum* bafflestone. (b) *Syringopora* bafflestone and framestone. (c) *Siphonodendron* bafflestone and framestone. (d) *Kueichouphyllum* framestone and *Kueichouphyllum*-*Syringopora* framestone. (e), (f), (g), (h) Bioclastic floatstones. Bra: Brachiopod, Bry: Bryozoan, C: Crinoid,

784 CA: Calcareous algae, G: Gastropod, K: *Kueichouphyllum*, M: Microbe, O: Ostracod, Si:
785 *Siphonodendron*, Sy: *Syringopora*.
786
787 Fig. 10. Thin-section micrographs of microfacies types and sedimentary structures in the coral
788 biostrome and its underlying and overlying limestones. (a) Wackestone in the biostrome. (b)
789 Packstone in the underlying limestone. (c) Packstone in the overlying limestone. (d) Packstone in
790 the overlying limestone. (e) Geopetal structure in the biostrome. (f) Burrow structure in the
791 biostrome. (g), (h) Boring structures in the biostrome. B: Burrows, Bra: Brachiopod, C: Crinoid
792 ossicle, CA: Calcareous algae, F: Foraminifer, FP: Fecal pellets, K: *Kueichouphyllum*, O:
793 Ostracod, P: Palaeoberesellid, Si: *Siphonodendron*.
794
795 Fig. 11. Model for sea-level changes controlling the growth and demise of the coral biostrome. (a)
796 Bioclastic limestones developed during low sea level. (b) Coral biostrome grew when sea level
797 rose. (c) Sea-level fall caused the demise of the coral biostrome and the development of bioclastic
798 limestones.
799
800 Fig. 12. Palaeogeographical locations of coral biostromes in western Europe, North Africa and
801 South China during the Viséan. 1: England and Ireland, 2: Belgium, 3: Spain, 4: Morocco, 5:
802 South China.
803
804 Table 1. Semi-quantitative analysis of compositions of biostrome-dwellers, microfacies types and
805 sedimentary structures in the coral biostrome and its underlying and overlying limestones in the
806 YS-A, YS-B and YS-C sections.
807
808 Table 2. Comparisons of coral biostromes between South China and Europe and North Africa.
809 Information about *Siphonodendron* biostromes in Belgium, SE Ireland, NW Ireland, SW Spain,
810 England and Morocco is taken from Aretz, 2001, 2002, Somerville et al., 2007, Aretz et al., 2010,
811 Rodríguez, 1996, Aretz and Nudds, 2007 and Said et al., 2010, respectively.
812

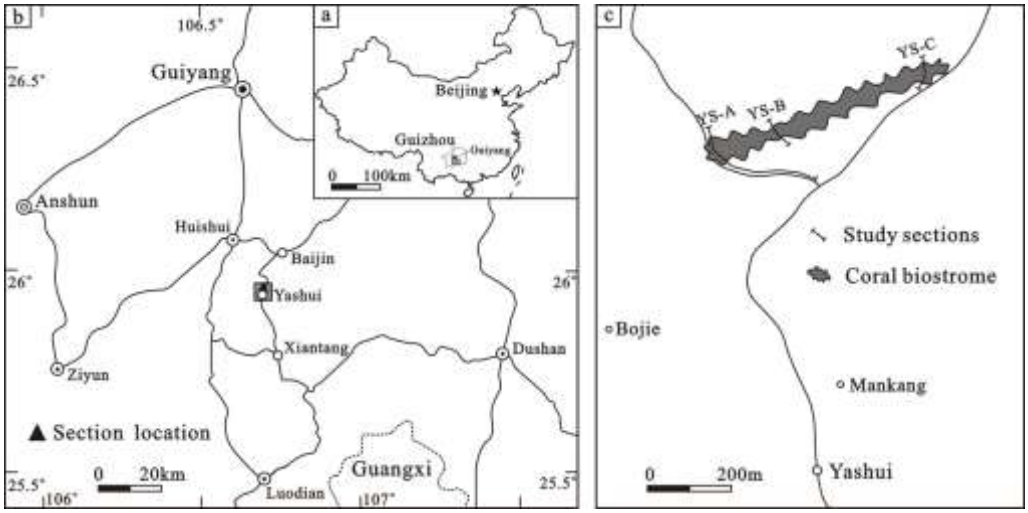
b
106.5°
26.5°
Guiyang
Anshun
Huishui
Baijin
Yashui
26°
Xiantang
Dushan
Ziyun
Section location
0 20km
25.5°
106°
Luodian
Guangxi
107°
a
Beijing
Guizhou
Guiyang
0 100km
c
YS-A
YS-B
YS-C
Study sections
Coral biostrome
Bojie
Mankang
0 200m
Yashui

Fig. 1

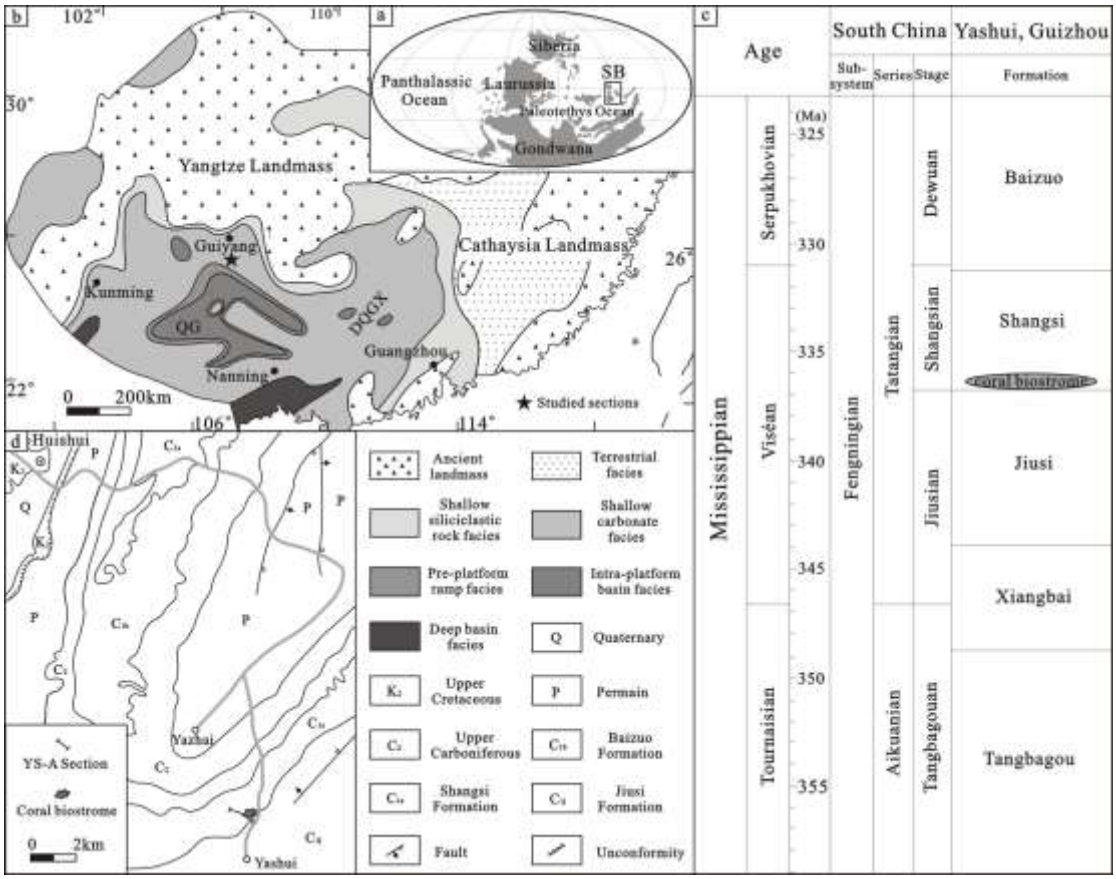
b
102°
110°
30°
Yangtze Landmass
Guiyang
Kunming
QG
DGCX
Guangzhou
Nanning
22°
0 200km
106°
114°
a
Siberia
SB
Panthalassic Ocean
Laurussia
Paleotethys Ocean
Gondwana
Cathaysia Landmass
26°
Studied sections
c
Age
South China
Yashui, Guizhou
Sub-system
Series
Stage
Formation
(Ma)
325
330
335
340
345
350
355
Mississippian
Serpukhovian
Visean
Tournaisian
Fengningian
Tatangian
Aikuanian
Dewuan
Shangsian
Jiusian
Tangbagouan
Baizuo
Shangsi
coral biostrome
Jiusi
Xiangbai
Tangbagou
d Huishui
Yazhai
Yashui
YS-A Section
Coral biostrome
0 2km
Ancient landmass
Terrestrial facies
Shallow siliciclastic rock facies
Shallow carbonate facies
Pre-platform ramp facies
Intra-platform basin facies
Deep basin facies
Quaternary
Upper Cretaceous
Permain
Upper Carboniferous
Baizuo Formation
Shangsi Formation
Jiusi Formation
Fault
Unconformity

Fig. 2

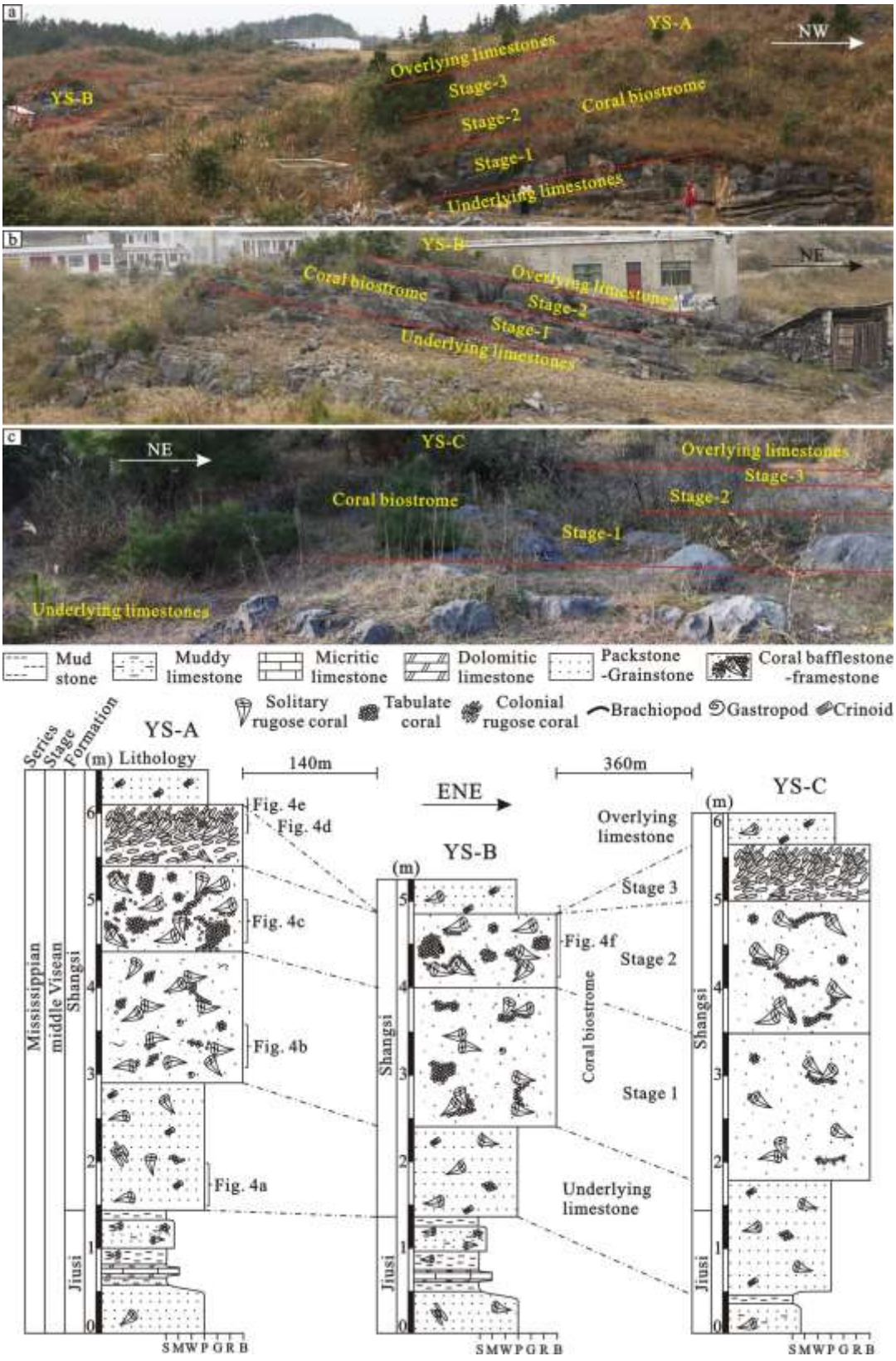
a
YS-A
NW
YS-B
Overlying limestones
Stage-3
Stage-2
Coral biostrome
Stage-1
Underlying limestones
b
YS-B
NE
Coral biostrome
Overlying limestones
Stage-2
Stage-1
Underlying limestones
c
NE
YS-C
Overlying limestones
Stage-3
Coral biostrome
Stage-2
Stage-1
Underlying limestones
Mud stone
Muddy limestone
Micritic limestone
Dolomitic limestone
Packstone -Grainstone
Coral bafflestone -framestone
Solitary rugose coral
Tabulate coral
Colonial rugose coral
Brachiopod
Gastropod
Crinoid
Series
Stage
Formation
YS-A
(m) Lithology
140m
ENE
360m
YS-B
YS-C
Fig. 4e
Fig. 4d
Fig. 4c
Fig. 4b
Fig. 4a
Fig. 4f
Overlying limestone
Stage 3
Stage 2
Stage 1
Coral biostrome
Underlying limestone
Mississippian
middle Visean
Shangsi
Jiusi
S M W P G R B

Fig. 3


a
b
T
SB
c
SB
T
d
SB
CR
e
Overlying limestone
Stage 5
CR
f
Overlying limestone
Stage 5
T
CR

Fig. 4

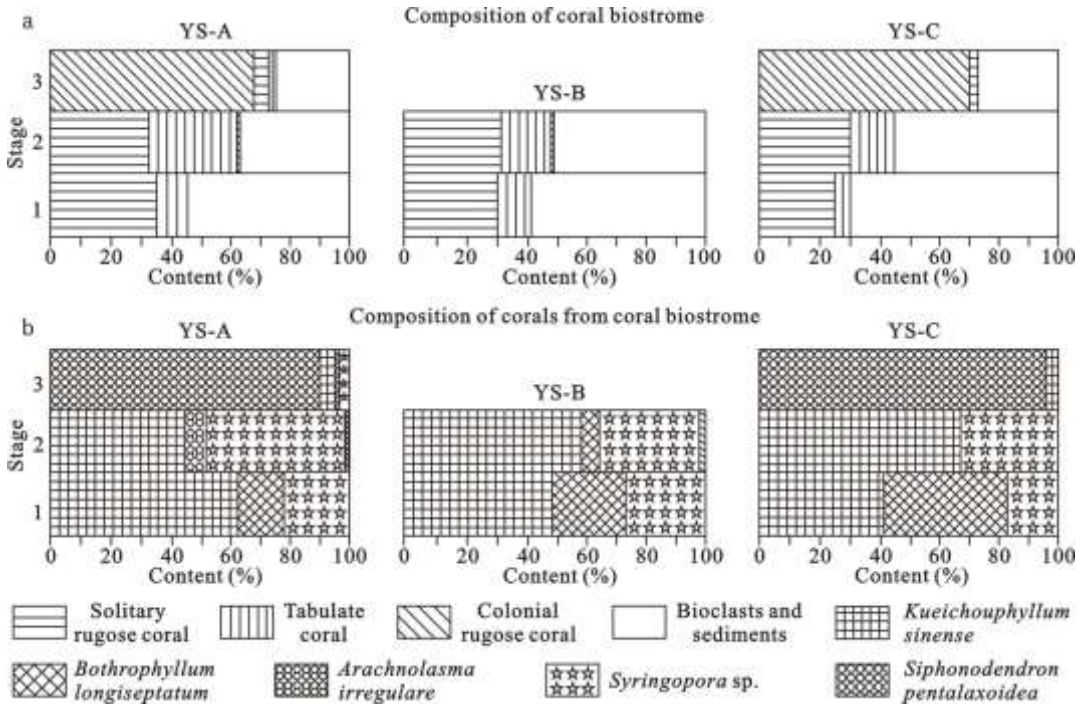
a
Composition of coral biostrome
YS-A
YS-B
YS-C
Stage
Content (%)
b
Composition of corals from coral biostrome
Solitary rugose coral
Tabulate coral
Colonial rugose coral
Bioclasts and sediments
Kueichouphyllum sinense
Bothrophyllum longiseptatum
Arachnolasma irregulare
Syringopora sp.
Siphonodendron pentalaxoidea

Fig. 5

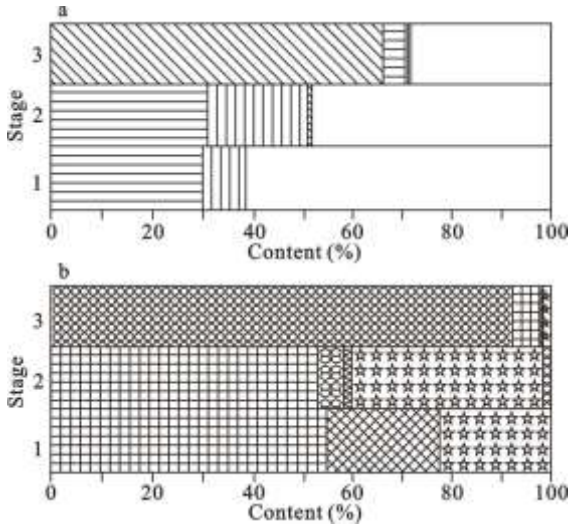
a
b
Stage
Content (%)

Fig. 6

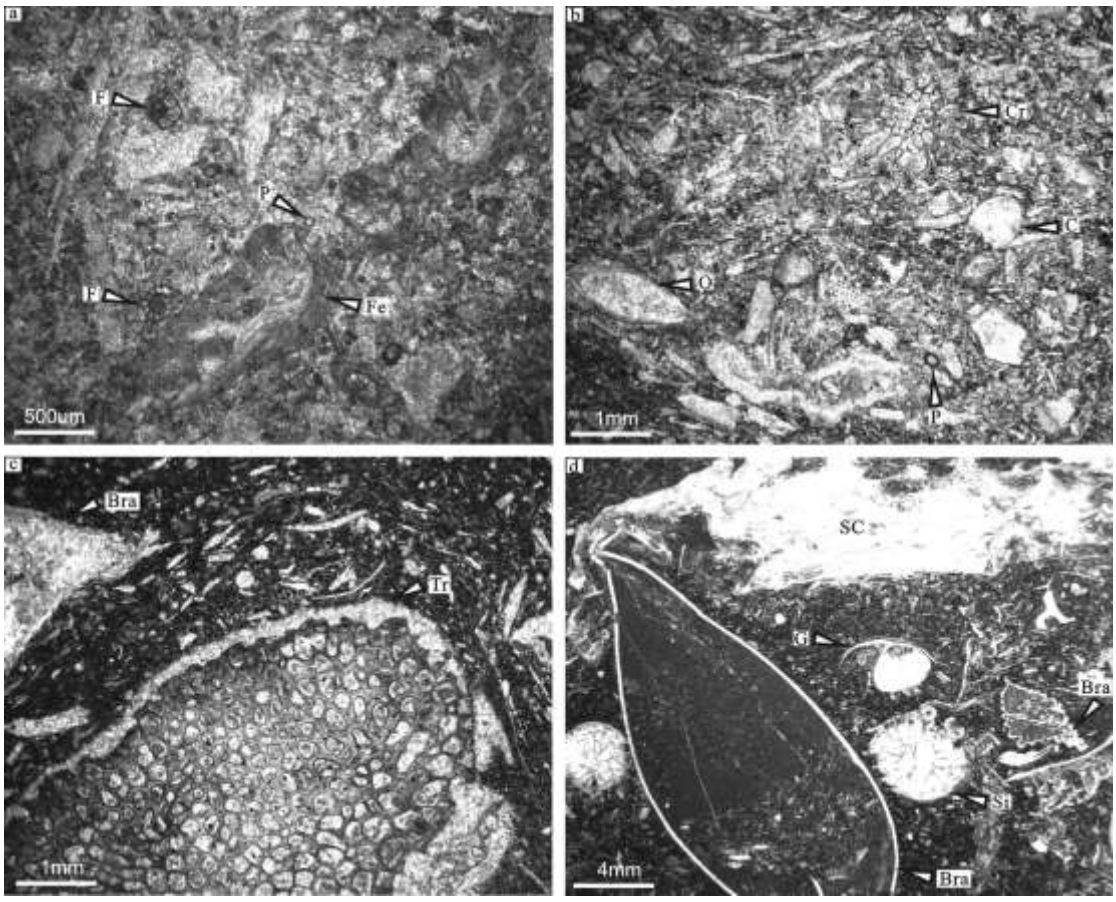

Fig. 7

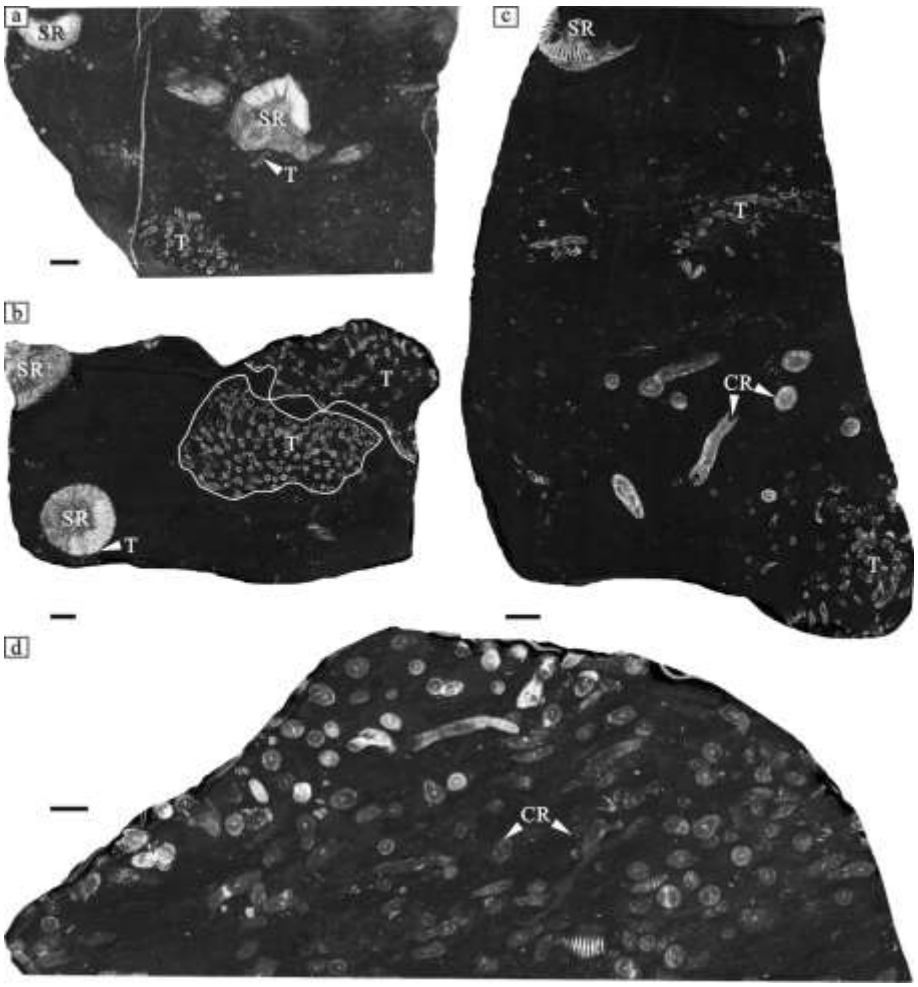

Fig. 8

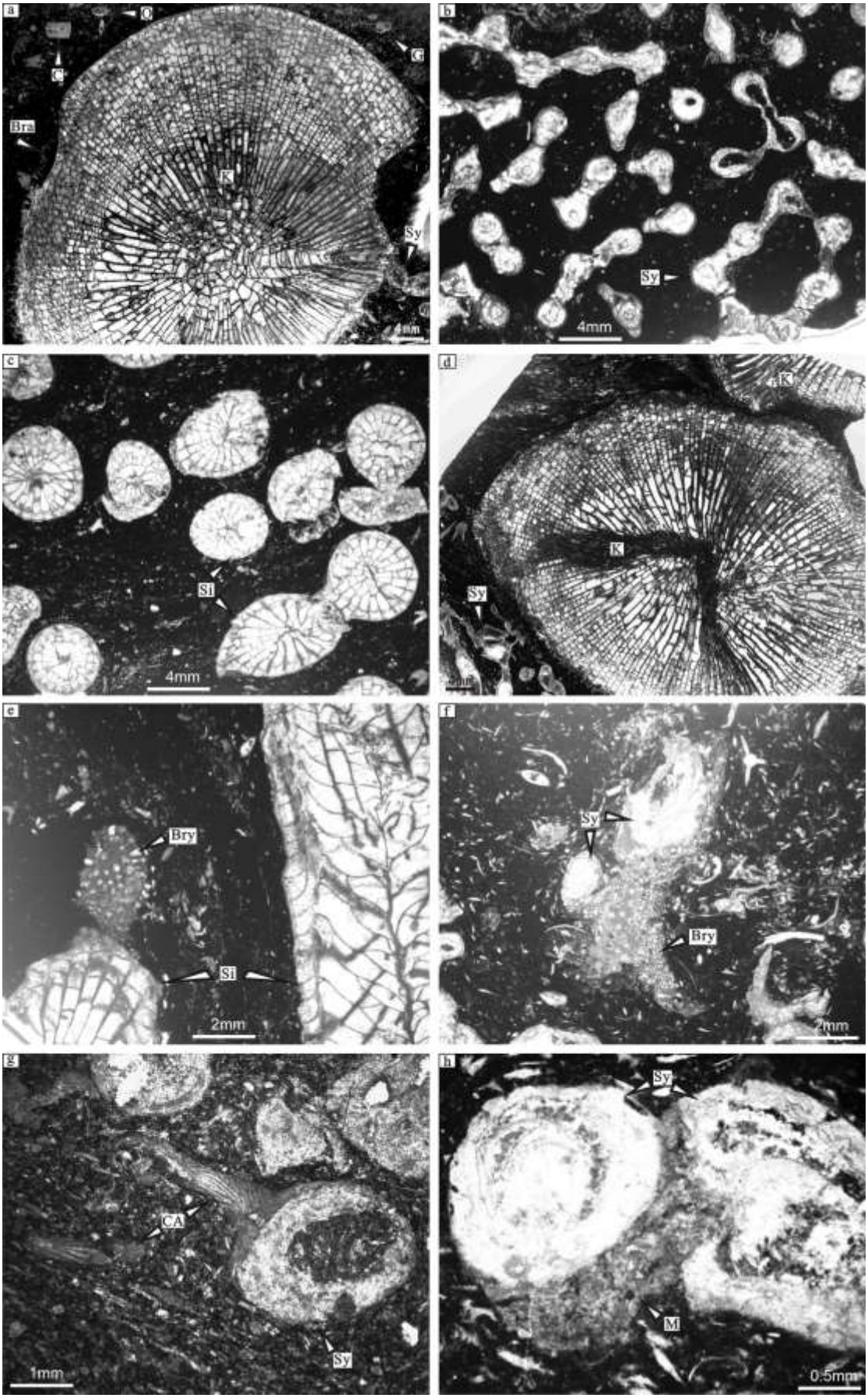
a
C
C
C
Bra
K
Sy
4mm
b
Sy
4mm
c
Si
4mm
d
K
K
Sy
e
Bry
Si
2mm
f
Sy
Bry
2mm
g
CA
Sy
1mm
h
Sy
M
0.5mm

Fig. 9

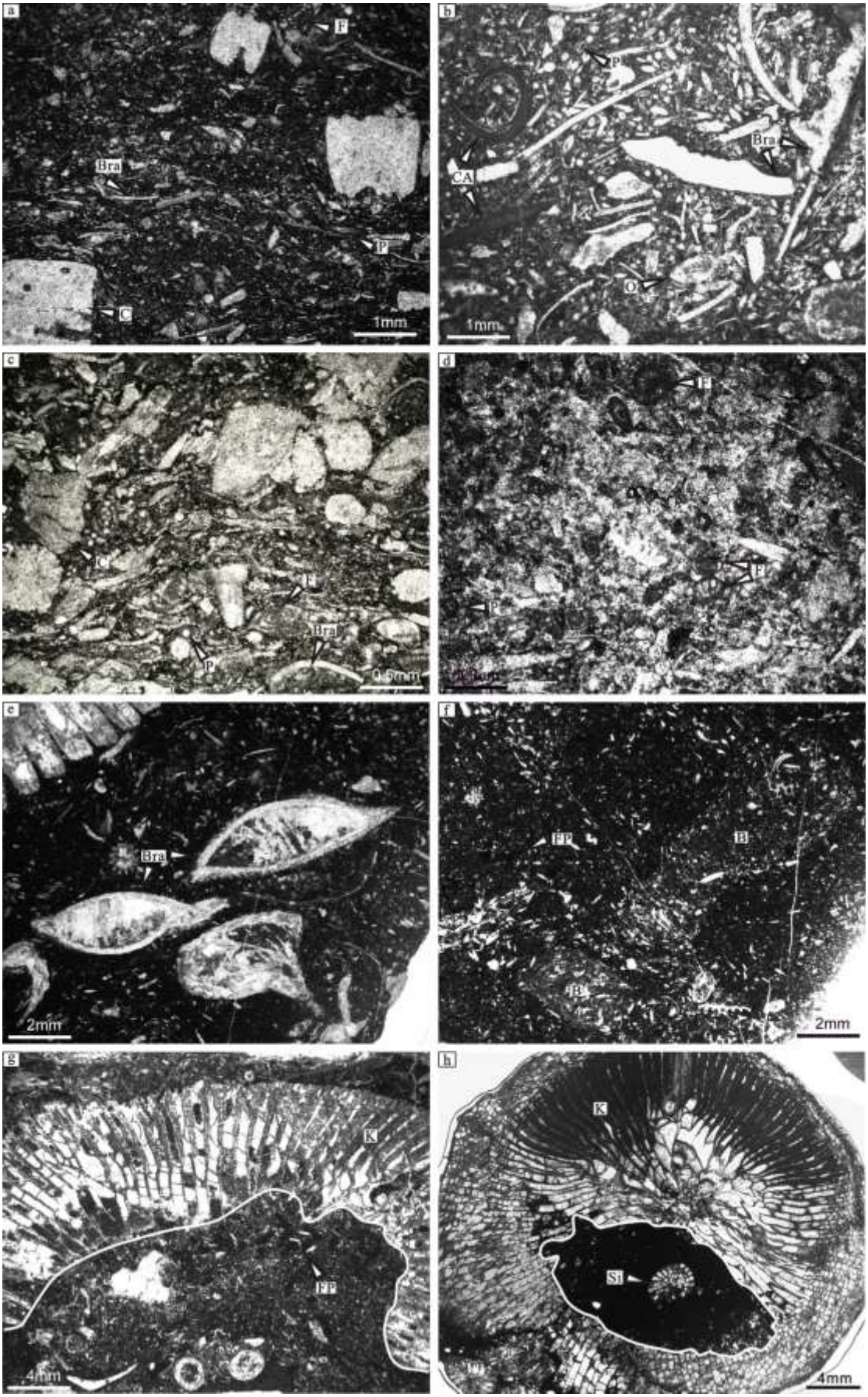
a
F
Bra
P
C
1mm
b
P
Bra
CA
Q
1mm
c
C
F
Bra
P
0.5mm
d
F
F
P
e
Bra
2mm
f
FP
B
B
2mm
g
K
FP
4mm
h
K
St
4mm

Fig. 10

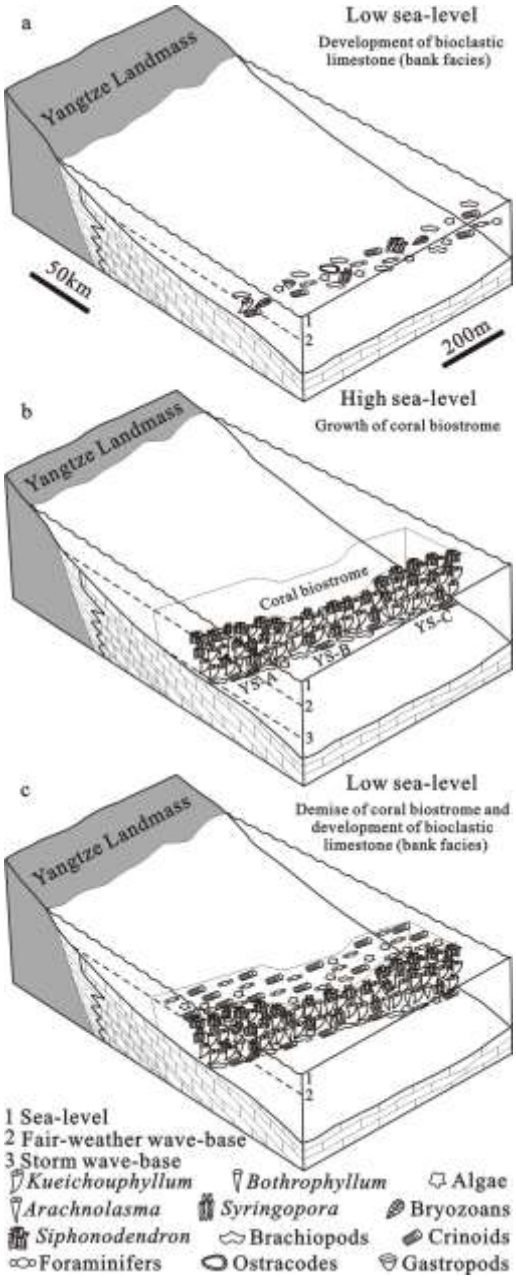
a
Low sea-level
Development of bioclastic limestone (bank facies)
Yangtze Landmass
50km
200m
1
2
b
High sea-level
Growth of coral biostrome
Yangtze Landmass
Coral biostrome
YS-A
YS-B
YS-C
1
2
3
c
Low sea-level
Demise of coral biostrome and development of bioclastic limestone (bank facies)
Yangtze Landmass
1
2
1 Sea-level
2 Fair-weather wave-base
3 Storm wave-base
Kueichouphyllum
Bothrophyllum
Algae
Arachnolasma
Syringopora
Bryozoans
Siphonodendron
Brachiopods
Crinoids
Foraminifers
Ostracodes
Gastropods

Fig. 11

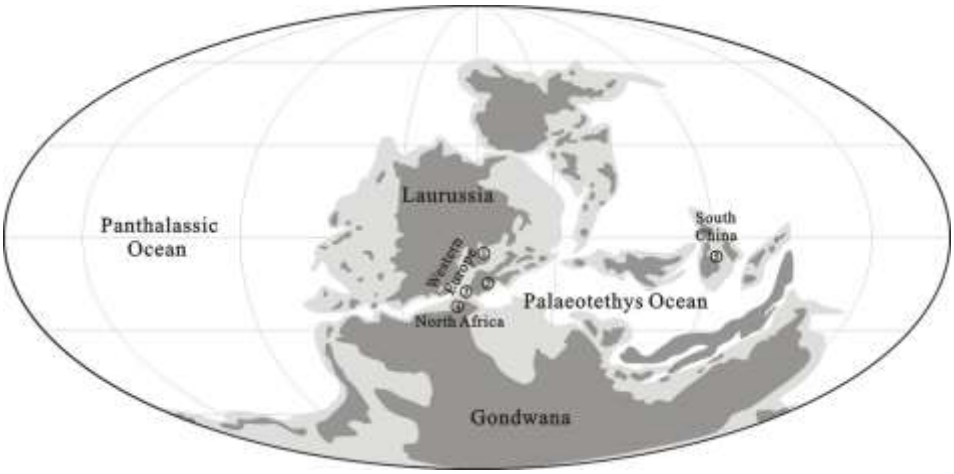

Fig. 12

		Composition of coral biostrome-dwellers						
		Brachiopods	Crinoids	Foraminifers	Calcareous algae	Gastropods	Bryozoans	Ostracods
YS-A	Stage 3	++	+	+	++	+	+	
	Stage 2	+++	++	+	+	+	++	+
	Stage 1	+++	++	++	+	+	+	+
YS-B	Stage 2	+++	+	+	+	+	+	+
	Stage 1	+++	++	++	+	++	+	++
YS-C	Stage 3	++	+	+	+	+	+	
	Stage 2	++	++	+	+	+	+	+
	Stage 1	+++	++	+	+	+	+	+

	Microfacies types					Sedimentary structures		
	Wackestone	Packstone	Floatstone	Bafflestone	Framestone	Burrow	Boring	Geopetal structure
Overlying limestone		+++				+		
Stage 3			+	+++	+++	+	+	+
Stage 2	+++	+	+	+++	++	++		+
Stage 1	++	++	+	+++	+	++	+	+
Underlying limestone		+++				+++	+	

+++ abundant, ++ common, + rare

Table 1

Locations	South China (this study)	Europe									North Africa
		Belgium			SE Ireland	NW Ireland			SW Spain	England	Morocco
Biostrome	*Kueichouphyllum -Syringopora -Siphonodendron* biostrome	*Siphonodendron* biostrome			*Siphonodendron* biostrome	*Siphonodendron* biostrome			*Siphonodendron* biostrome	*Siphonodendron* biostrome	*Siphonodendron* biostrome
		Martini biostrome	*Junceum* biostrome	*Junceum-martini* biostrome		*Pauciradiale* biostrome	*Martini* biostrome	*Junceum* biostrome			
Biostrome type	Autobiostromes	Parabiostromes	Autobiostromes	Autobiostromes	Autobiostromes	Parautobiostromes	Parabiostromes and autoparabiostromes	Autobiostromes	Autobiostromes	Parabiostromes	Autoparabiostromes
Thickness	Thick (2.5-3.9m)	Thin (0.2-0.5m)	Thin (0.42m)	Medium (0.6-0.8m)	Medium (1-2.5m)	Very thick (8-50m)	Very thick (5-10m)	Very thick (5-10m)	Very thick (6-20m)	Medium (0.5-1m)	Thick (2-5m)
Coral diversity	Low (5species)	Low	Low (6 species)	Middle (10 species)	Low–high (5–14 species)	Low–high (4–13 species)	High (11 species)	Very low–moderate (1–7 species)	Middle (9 species)	Middle (8 species)	High (24 species)
Dominant species	*S. pentalaxoidea, Syringopora* sp., *K. sinense,*	*S. martini*	*S. junceum, Lithostrotion maccoyanum, S. pauciradiale, Syringopora* sp.	*S. junceum, S. martini*	*S. pauciradiale*	*S. pauciradiale, Solenodendron furcatum*	*S. martini, S. pauciradialeor, S. sociale*	*S. junceum*	*S. martini, S.irregulare, Syringopora*	*S.* spp.	*S. junceum*
Solitary corals	*K. sinense Bothrophyllum longiseptatum, Arachnolasma irregulare,*	No solitary corals	No solitary corals	*Aulophyllum fungites, Dibunophyllum bipartitum, Koninckophyllum* sp.	*Axophyllum vaughani, Aulophyllum fungites, Dibunophyllum bipartitum, Palaeosmilia murchisoni, Pseudozaphrentoides juddi*	*Axophyllum* sp., *A. pseudokirsopianum, Caninophyllum archiaci, Dibunophyllum* sp. *Haplolasma* cf. *densum, Siphonophyllia samsonensis, S. siblyi*	*Caninophyllum archiaci, Clisiophyllum sp. Haplolasma* cf. *densum, Palaeosmilia murchisoni, Siphonophyllia* cf. *siblyi*	*Caninophyllum archiaci, Clisiophyllum garwoodi, Dibunophyllum* sp., *Pseudozaphrentoides juddi, Siphonophyllia* sp.,	*Axophyllum vaughani, A. densum, A.* sp., *A.* cf. *pseudokirsopianum, Clisiophyllum garwoodi, Dibunophyllum bipartitum*	*Axophyllum vaughani, Caninophyllum archiaci, Siphonophyllia siblyi*	*Arachnolasma, Axophyllum, Clisiophyllum, Dibunophyllum, Koninckophyllum, Palaeosmilia,*
Distinctive associated biota	Crinoids, brachiopods, foraminifers, calcareous algae bryozoans, ostracods, gastropods	Crinoids, brachiopods, foraminifers	Crinoids, foraminifers, bryozoans	Crinoids, brachiopods, foraminifers, algae, gastropods	Crinoids, foraminifers (locally common), dasycladacean algae (locally common), bryozoans (rare),	Brachiopods, bryozoans	Crinoids, bryozoans, foraminifers (rare), dasyclads (rare)	Brachiopods, red algae, green algae (rare)	Brachiopods (abundant), crinoids, foraminifers, calcareous algae, bryozoans, ostracods, molluscs	Crinoids, foraminifers, pelmatozoan, gastropods	Crinoids, foraminifers, algae, cyanobacteria, ostracods, trilobites
Proportion of in situ colonies	high (>60%)	Low (<20%)	High (>60%)	High (>60%)	High (>60%) (Bannagogle Guarry section)	Low–high ([5–]10–50%)	Low (10–15%)	High (>50%)	High (>60%)	Very low (<2.5%)	Low–high (20–60%)
Degree of fragmentation	Low	High	Low	Low	Low	Moderately low –very high	High	Low	Low	Very high	Low
Depositional environment interpretation	Formation between storm wave-base and fair-weather wave-base	Formation above fair-weather wave-base	Formation between storm wave-base and fair-weather wave-base	Formation between storm wave-base and fair-weather wave-base	Formation between storm wave-base and fair-weather wave-base	Formation between storm wave-base and fair-weather wave-base	Formation above fair-weather wave-base	Formation mostly below storm wave-base but with occasional short-lived shallowing events	Formation between storm wave-base and fair-weather wave-base	Formation above fair-weather wave-base	Formation between storm wave-base and fair-weather wave-base

Table 2